Environmental Advances 8 (2022) 100241

Contents lists available at ScienceDirect

Environmental Advances

journal homepage: www.sciencedirect.com/journal/environmental-advances

# Critical evaluation of the chemical composition of acid mine drainage for the development of statistical correlations linking electrical conductivity with acid mine drainage concentrations

Janet Smith [a,b,d,*], Craig Sheridan [a,c], Lizelle van Dyk [a,b], Kevin G. Harding [a,b]

[a] Centre in Water Research and Development, University of the Witwatersrand, Johannesburg, Private Bag 3, Wits 2050, South Africa
[b] School of Chemical and Metallurgical Engineering, University of the Witwatersrand, Johannesburg, Private Bag 3, Wits 2050, South Africa
[c] School of Geography, Archaeology and Environmental Studies, University of the Witwatersrand, Johannesburg, Private Bag 3, Wits 2050, South Africa
[d] CM Solutions Metallurgical Consultancy and Laboratories (Pty) Ltd, Pinelands Office Park, Unit T5, 1 Ardeer Road, Modderfontein 1609, South Africa

ARTICLE INFO

*Keywords:*
Physio-chemical composition
Electrical conductivity
Correlation
Regression equations

ABSTRACT

The design an effective treatment processes for the remediation of acid mine drainage (AMD) requires an understanding of the composition of the AMD water. The pH and elemental composition of AMD waters are site specific and are dependent on the regional geology, and environmental factors. To establish the chemical and physical characteristics of two AMD sites located in the Mpumalanga coal mining region, South Africa, samples were taken between February 2018 to April 2019. These data were compared against regulatory legislation, and the potential health effects of exposure indicated. Strong correlations were noted between parameters and statistical evaluation demonstrated that electrical conductivity (EC) could be a useful correlative for prediction of total acidity, dissolved iron, and sulfur concentrations in acidic AMD waters. From these findings, empirical correlations were used to derive regression equations which were used to derive the EC values corresponding to the respective water quality limits for total dissolved solids (TDS), dissolved iron, and sulfur to provide a rapid method for testing compliance. Given the site specificity of AMD composition, this approach is intended as a proof of concept for the development of a methodology for adaption at other AMD sites. The regression equations should not be considered as universal to all AMD sites and EC should also not be used as a replacement for more complete chemical analysis.

## Introduction

The uncontrolled decant of acid mine drainage (AMD) is one of the most pressing global environmental challenges facing gold and coal mining operations (Gazea et al., 1996, Geosciences, 2016, Simate and Ndlovu, 2014). Exposure of sulfide-bearing ores to oxygen and water results in the formation of AMD, which is characterised by low pH and comprises significantly elevated concentrations of iron and sulfate. The low pH promotes secondary reactions which could cause the dissolution of other trace metals in the AMD depending on the regional geology, temperature, pH, availability of micro-organisms, presence of acid neutralising chemicals, oxygen and water . The overall reaction for the weathering of pyrite to form AMD is given in Eq. 1 (Akcil and Koldas, 2006, Banks et al., 1997, Nordstrom et al., 2015, Simate and Ndlovu, 2014).

$$4FeS_2 + 15O_2 + 14H_2O \rightarrow 4Fe(OH)_3\downarrow + 8SO_4 + 16H \quad (1)$$

The pollution loads in surface waters, streams and rivers draining the Witwatersrand gold mining region were previously assessed and the impact of the spatial distribution, seasonality, and chemical processes of these AMD waters are well understood (Davidson, 2003, Marsden, 1986, Tutu et al., 2008). The South African Department of Minerals and Energy (DMR) website lists a total of 126 operating coal mines in the Mpumalanga region (DMR, 2017) (Fig. 1).

The Witbank coalfield extends from Springs to Belfast in the upper Olifants catchment which is shown as Fig. A1 in Appendix A of the supplementary material. The Water Research Commission, (WRC) has considered the entire Olifants River Water Management area as highly

* Corresponding author at: CM Solutions Metallurgical Consultancy and Laboratories (Pty) Ltd, Pinelands Office Park, Unit T5, 1 Ardeer Road, Modderfontein 1609, South Africa
*E-mail address:* janetsmith.solutions@gmail.com (J. Smith).

https://doi.org/10.1016/j.envadv.2022.100241
Received 27 April 2022; Received in revised form 4 May 2022; Accepted 6 May 2022
Available online 7 May 2022

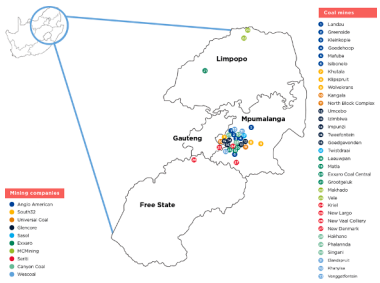


**Fig. 1.** Location of coal mines in South Africa (MinteralscouncilSouthAfrica, 2019).

stressed with limited opportunity for further water resource development (WRC, 2015). Decant from coal mining sites in the Witbank Middelburg area flows into tributaries of the Olifants River causing significant increases in the salinity and sulfate levels of nearby dams thus deleteriously affecting the quality of local watercourses (McCarthy, 2011). Furthermore, the coalfields in this area are classified as posing a significant AMD risk, which results in a medium to high mineralogical risk depending on the local surface water neutralisation capacity (WRC, 2015). Adding to these risks are the poor mine decommissioning efforts, which in the past, were characterised by insufficient closure planning and the underestimation of potential post-closure environmental liability.

Treatment of AMD would avert further pollution of local watercourses and also address historic liability issues. The re-use of AMD was an option proposed by the Honorable Nomvula Mokonyane for "Improving the water mix" in her budget vote speech in May 2015 (DWS, 2017). Design of adequate, robust remediation facilities requires an understanding of the chemical characteristics of the AMD waters and the extent to which seasonal variation affects contaminants, and the re-use of remediated AMD for mining processes, crop irrigation, or domestic use would be dependent on the quality of water achieved.

With this in mind, two AMD sites in the Mpumalanga region were monitored to quantify seasonal physio-chemical parameters during 2018/2019. Smith et al. (2021) noted that increased rainfall volumes coincided with decreased parameter concentration thus confirming seasonal variability. As expected, total dissolved solids (TDS), and electrical conductivity (EC), and total ion values were correlated (Smith et al., 2021). The focus of this present paper was to extend the comparison to include a correlation matrix for all parameters analysed and to apply statistical evaluation to evaluate the extent of the relationships between the variables.

## Method

### *Sampling and preservation*

Approximately monthly sampling from two AMD dams between February 2018 and December 2018, with an additional samle taken in April 2019, resulted in a total of thirteen samples collected from Site 1, a receiving dam for AMD waste from local coal mines, and six samples from Site 2, a dam constructed to collect immediate operational runoff, in the Mpumalanga coalfields region, South Africa. Restricted access to site 2, limited more frequent sampling from this AMD dam. Surface water grab samples were collected in glass or polypropylene (PP) containers and transported back to the School of Chemical and Metallurgical Engineering at the University of the Witwatersrand, Johannesburg. As per the requirements of the American Public Health Association (APHA) Standard Methods for the Examination of Water and Wastewater, a 50 mL portion of each sample was filtered through a 0.45 μm filter and preserved with ultrapure nitric acid to achieve a pH of less than 2 for dissolved metals analysis (APHA et al., 2005). This, and the remaining samples, were stored at 4 °C. Except for inductively coupled plasma (ICP) analysis, all analyses were conducted at the School facilities. ICP analysis was subcontracted to various laboratories which included: The University of the Witwatersrand School of Chemistry (Wits Chem), De Bruyn Spectroscopic (DBS), and University of Johannesburg analytical department (UJ). The limitations around acquiring ICP:OES data from different laboratories, are acknowledged, given that different instrumentation models were used, and different technicians were responsible for conducting the ICP:OES analyses, however, not withstanding these limitations, the authors believe that the data and extrapolations drawn from these, are valid.

### *Analytical methods*

The analytical methods used, and the instrumentation models are given in Table 1.

### *Calibration and data quality control*

The pH electrode was calibrated using three buffer solutions at pH 4, 7 and 10. Measurement of a pH 4 control sample was within 0.05 pH units. The conductivity electrode was checked against 1413 μS/cm and 12.88 mS/cm reference solutions before use, the Eh electrode was checked against Eh 475 mV standard buffer solution before measurement and the turbidimeter meter was checked against standard solutions before use. In all instances, readings were within 5 % of the standard value. An error of 1.2 % was shown from repeat analyses of an acidity control sample. Inductively Coupled Plasma Optical Emission Spectroscopy (ICP) standards were prepared using certified standards and all solutions were prepared using deionized, Milli-Q, 18 MΩ water. Analytical-grade nitric acid was used for sample dilutions and a matrix-matched sample blank was determined to quantify any background contaminants that might exist. As a quality control check, TDS, EC, and the sum of the total ions were compared for agreement and cation/anion balances were calculated to confirm the electrical neutrality of the samples. Six of the samples analysed reported cation/anion balances of less than 5%. Ten samples reported cation/anion balances between 5% and 9%, and the remaining 3 samples recorded cation/anion balances above 10%. In most instances, a negative value was reported indicating a possible under-reporting of cations or an over-reporting of anions. The

**Table 1**
Methodology and/or instrumentation used for sample analysis.

| Parameter | Instrumentation |
|---|---|
| pH | Ohaus ST3-100 combined pH and mV meter and ST310 pH electrode with an integrated temperature probe. |
| Conductivity (EC) | Ohaus ST3-100C conductivity meter and STCON3 electrode. |
| Redox Potential (Eh) | Ohaus ST3-100 combined pH and mV meter using a STORP1 redox probe and STREF 2 saturated calomel reference probe. Eh values were reported relative to the standard hydrogen electrode (SHE). |
| Total dissolved solids (TDS) | Gravimetric determination with filtration using GF filter paper followed by drying of filtrate in a Memmert drying oven at 180 °C to constant mass. |
| Total suspended solids (TSS) | Gravimetric determination with filtration using GF filter paper followed by drying in a Labotec EcoTherm drying oven at 105 °C to constant weight. |
| Turbidity (NTU) | HACH-2100N Turbidimeter. |
| Alkalinity/acidity (TA) | Potentiometric titration to pH 8.3 for acidity and pH 4.5 for alkalinity, using 1.0 M NaOH and 0.02 M $H_2SO_4$ for acidity & alkalinity, respectively. Acidity titrations were preceeded by the addition of hydrogen peroxide oxidation and heating to oxidise any metals present in the samples. |
| Anions (S) | Sulfur determined using ICP-OES and sulfate concentration calculated assuming all S present as $SO_4^{2-}$ ion. |
| Metal(loids) | Inductively Coupled Plasma Optical Emission Spectroscopy (ICP-OES) - Spectro Genesis, model Genesis Fee - Wits Chem; ICP-OES - Spectro Arcos (SOP) – UJ, and SPECTRO CIROS CCD Vacuum ICP-OES – DBS. |

higher cation/anion balances observed for Site 1 coincided with significantly increased rainfall events in March, October, and November, where dilution effects might have resulted in the under-reporting of cations. The higher cation/anion balances observed for Site 2 coincide with high acidity values observed in May and August. The reduced pHs and increased Fe concentrations reported during this time, would indicate increased AMD formation, which, with the reduced Ca concentrations observed, would have upset the buffering capacity of the water and as such impacted the chemical balance.

*Comparison of data with legislative and advisory guides*

Data for the dissolved metals analysis were compared against legislative and advisory guides for drinking water, which included: the South African National Standard - SANS 241-1:2015 Drinking Water Specification (SABS, 2015); SANS 241:2006 (Ed.6) Drinking Water Quality Requirements (SABS, 2006); the United States Environmental Protection Agency (EPA) 2018 Edition of the Drinking Water Standards Health Advisories Maximum Contaminant Level (MCL) and Drinking Water Equivalent Level (DWEL) (EPA, 2018); and the Department of Water Affairs (DWAF) 1996 Water Quality Guidelines for Domestic Use Target Water Quality Range (TWQR) (DWAF, 1996).

## Results and discussion

*Analytical data*

All data for the physical and chemical parameters as well as the dissolved metals ICP:OES analysis data are reported in the supplementary material, Appendix B, Tables B1-B9. Parameters found in excess of prescribed legislative limits are given in Table C.1-C.4 in Appendix C of the supplementary material.

Acidic pH values of less than pH 3 were reported for all sampling events, and except for the April 2019 site 2 sample, where a pH of 7 was recorded. TA concentrations are comprised of free protons, and hydrolysable metals such as iron (Fe), manganese (Mn), and aluminium (Al) (Cravotta III and Kirby, 2004). The variation in TA concentration between the two sites is attributed to differing concentrations of metals present in the respective AMD waters. TA is not subject to legislative control, but can contribute significantly to the corrosiveness of water, and the hydrolysable salt contribution to the TA concentration, also constitutes a serious pollution problem (Cravotta III and Kirby, 2004, Larson and Henley, 1955). EC, TDS, Fe, and sulfur (S) concentrations were all in excess of legislative limits, and recorded significantly higher concentrations for site 1. Calcium (Ca), magnesium (Mg), manganese (Mn), and nickel (Ni) reported concentrations in excess of legislative limits, but with smaller concentration differences between site 1 and 2. With the exception of the April sample for site 2, Al, beryllium (Be), cadmium (Cd), and lead (Pb) concentrations reported concentrations in excess of legislative limits. For site 1 and site 2, chromium (Cr), Uranium (U), and vanadium (V) reported some samples within, and some in excess of legistative limits. All boron (B) and zinc (Zn) concentrations for site 2 were below the required legislative limits. With the exception of one sample, all Zn concentrations from site 1 were in excess of legislative limits, and 4 of the 11 samples analysed for B, were outside of legislative limits.

*Potential health effects*

While some metals such as Ca, Co, Cr, Cu, Fe, Mg, Mn, molybdenum (Mo), Ni, and Zn are essential to human and plant health, long-term exposure to concentrations of certain elements over regulatory or advisory levels, or deficiencies in some, could lead to potential health and/or environmental effects (Kyerematen, 2013, Smith, 2007).

Low pH levels result in increased dissolution of metals and metalloids from the surrounding geology and the increased mobility of these potential contaminants into the environment (Smith, 2007). Hydolysis of metals such as Fe, Mn and Al contribute to elevated TA concentrations, which can have significant environmental and corrosive effects owing to increased TDS concentrations and the toxicity of its contributory ions (Cravotta III and Kirby, 2004). Infiltration of this acidic run-off into watercourses, could cause harm to aquatic systems, negatively impact surrounding vegetation, and, if ingested, cause health issues in humans and animals (DWAF, 1996). High sulfate concentrations could affect health, contribute to corrosion, and could also cause increased sediment levels in water bodies as a result of pH and chemistry changes resulting in precipitation (DWAF, 1996). The potential health effects of elements present in excess of legislative control concentrations, are summerised in Appendix D, Tables D1-D2 (EPA, 2018, DWAF, 1996).

*Seasonal variability*

Smith et al. (2021) confirmed that AMD sites were subject to seasonal variability, based on the reduction in TDS, and other parameter concentrations that coincided with increased rainfall volumes. Strong correlations were noted between EC, the calculated sum of the total ions, and the gravimetrically determined TDS concentrations (Smith et al., 2021). Smith et al. (2021) also noted that other parameters followed similar trends to the TDS concentrations over time. This work explores the extent of these relationships.

*Correlation analysis*

The Microsoft Excel correlation analysis tool was used to extend the correlation matrix to include all chemical and physical parameters analysed for the two AMD sites. The correlation matrix was then narrowed to include only correlated parameters that were greater than ± 0.5 and common to both sites. Because of the ease of measuring EC, the correlation was further reduced to include only parameters that correlated with EC. These correlations were then exploited for development of a statistical correlation, for use as a screening tool that would link EC with major AMD concentrations. Regression coefficients were established to describe the mathematical equation of the regression line.

Dissolved K, was excluded from further statistical analysis as this parameter presented positive and negative correlations for site 1, and site 2 respectively, and reported significantly lower concentrations compared with other parameters. Remediation efforts at Site 2, resulted in the April 2019 sample presenting a neutral pH which was not representative of the original physio-chemical make-up of this AMD site and hence its omission from further statistical analysis.

Stronger correlations were observed for Site 2, and could be attributed to the lower ion concentration present in this AMD site, and/or because of the small sample size available for evaluation for this site, compared with the 13 data sets available for Site 1 (Smith et al., 2021). As both sites were located in close proximity, and as such, shared regional geology, both data sets were combined to broaden the correlation and give a statistically more robust sample. A pooled correlation was performed using the extended Excel data analysis tool at a 95 % confidence level. The individual and the pooled correlation coefficients are shown in Table 2.

As indicated by the correlation coefficient "*r*" approaching +1, the combined correlation data indicated strong positive correlations between all selected parameters (Hannigan and Lynch, 2013).

*Regression analysis*

To exploit the correlations observed between EC, TDS, TA, dissolved Fe and S, regression analyses were performed at a 95% confidence level, using the Excel data analysis tool with EC as the independent variable (*x*-value), and TDS, TA, Fe and S as the dependent variables (*y*- values). These data provided a measure of the extent to which the calculated regression analysis fits the source data (Cheusheva, 2019). The

**Table 2**
Separate and pooled correlations between electrical conductivity, calculated total dissolved solids, total dissolved solids, total acidity, dissolved iron and dissolved sulfur concentrations.

| **Correlation** | **R** | | | | | | | | | |
|---|---|---|---|---|---|---|---|---|---|---|
| **Parameter** | **EC** | | **TDS** | | **Sum of Total Ions** | | **Total Acidity** | | **Dissolved Fe** | |
| **Site** | **1** | **2** | **1** | **2** | **1** | **2** | **1** | **2** | **1** | **2** |
| EC | 1 | | | | | | | | | |
| TDS | 0.88 | 0.97 | 1 | | | | | | | |
| Sum of Total Ions | 0.67 | 0.88 | 0.55 | 0.91 | 1 | | | | | |
| TA | 0.96 | 0.98 | 0.85 | 0.93 | 0.75 | 0.91 | 1 | | | |
| Dissolved Fe | 0.63 | 0.90 | 0.51 | 0.88 | 0.99 | 0.97 | 0.70 | 0.95 | 1 | |
| Dissolved S | 0.70 | 0.92 | 0.57 | 0.93 | 1.00 | 1.00 | 0.77 | 0.94 | 0.99 | 0.98 |
| **Site** | **1 & 2** | | **1 & 2** | | **1 & 2** | | **1 & 2** | | **1 & 2** | |
| EC | 1 | | | | | | | | | |
| TDS | 0.9627 | | 1 | | | | | | | |
| Sum of Total Ions | 0.8712 | | 0.8350 | | 1 | | | | | |
| Total Acidity | 0.9912 | | 0.9570 | | 0.8974 | | 1 | | | |
| Dissolved Fe | 0.8810 | | 0.8394 | | 0.9953 | | 0.9039 | | 1 | |
| Dissolved S | 0.8829 | | 0.8474 | | 0.9993 | | 0.9089 | | 0.9935 | |

regression analysis output included regression statistics, an analysis of variance (ANOVA), and regression coefficients. These data are given in Table E.1 of Appendix E.

The ANOVA output, tests the significance of the correlation between the dependent and independent variables, and provides information on the regression model (Aydin, 2015). An *F*-critical value of 4.49 was calculated at a 95 % confidence level using the following equation.

$$\text{FCritical} = F.INV.RT(0.05,\ 1, 16) \tag{2}$$

The ANOVA output data are reported in Table 3, in the format; [$F(x, y) = a,\ p = b$]; where:

$x$ = degrees of freedom of the independent variable

$y$ = degrees of freedom of the dependent variable a = the *F- statistic* b = the *Significance F* or *P*-value of *F*

The statistical ouput showed that significance *F*, or the *p*-value of *F*, for all dependent variables, were less than 0.05 indicating a linear relationship between the independent variable EC and each of the dependent variables tested. In all instances, the *F*-statistic was greater than the calculated -critical value, indicating that the observed relationship between the dependent and independent variables did not ocour by chance. Thus the change in EC value, the independent variable, was statistically confirmed to describe the variation in the dependent variables; TDS, TA, dissolved Fe and dissolved S respectively (Mursau, nd).

The regression coefficients output are shown in Appedix E, Table E.2. The regression coefficients, describe the mathematical equation for the regression line, y =mx+b, and were calculated using the least-squares method, which calculates the slope (m) and intercept values (b) that achieve the smallest sum of the squares of the vertical variations of the determined concentrations from the predicted values in the regression line (Tripepi et al., 2008). The intercept value explains the theoretical concentration of the dependent ($y$) variable when the independent ($x$) variable is equal to zero (Tripepi et al., 2008, Yan and Su, 2009). The regression equation is used to calculate the probable concentration of the dependent ($y$) variable from the given value of the independent ($x$) variable (Tripepi et al., 2008, Yan and Su, 2009). A *t*-Critical value of 2.12 was calculated using the following equation (Mursau, nd)

$$\text{TCritical} = T.INV.2T(0.05,\ 1, 16) \tag{3}$$

**Table 3**
Summary of ANOVA test results at a 95 % confidence level.

| **Dependent Variable** | **Independent Variable** | **ANOVA Test Results** |
|---|---|---|
| TDS | EC | $[F(1,16) = 203,\ p = 1.67E^{-10}]$ |
| TA | EC | $[F(1,16) = 894, p = 1.18E^{-15}]$ |
| Fe | EC | $[F(1,16) = 56, p = 1.37E^{-06}]$ |
| S | EC | $[F(1,16) = 57, p = 1.23E^{-06}]$ |

The *t*-Statistic was greater than the *t*-Critical value for all parameters, confirming the overall significance of the model and the calculated *P*-value was less than 0.05 for all parameters, indicating that the relationship between the dependent and independent variables was significant. The upper and lower confidence intervals, which describe the upper and lower boundaries of the regression line, did not include zero within their range. Regression analysis confirmed that a linear relationship did exist between the dependent and independent variables. Thus EC could be used as a proxy to predict TDS, TA, dissolved S, and dissolved Fe concentrations in these AMD waters, provided a sufficiently large database was used to underlie the correlation. The linear regression Eqs. 4-7, were derived using the slope and intercept values, and may be used to estimate the concentrations of the dependent variables, namely; TDS, TA, dissolved Fe and dissolved S from the EC value. (Cheusheva, 2019, Tripepi et al., 2008). The units for the x-variable units are expressed in mS/m, and in mg/L for the y-variable.

$$\text{TDS} = 6.2384\ x\ -\ 963.45 \tag{4}$$

$$\text{TA} = 3.7910\ x\ -\ 3103.27 \tag{5}$$

$$Dissolved\ S = 1.2429\ x\ -\ 63.8190 \tag{6}$$

$$Dissolved\ Fe = 1.7878\ x\ -\ 2133.15 \tag{7}$$

The large intercept value observed in these regression equations would however limit the use of these equations for predictive purposes over a broad concentration range. To remedy this, the trendline intercepts were set to zero and a scatter plot of these data with their regression equations is shown in Fig. 2. The revised regression equations are given in the following equations.

$$\text{TDS} = 5.9524\ x \tag{8}$$

$$\text{TA} = 2.8703\ x \tag{9}$$

$$Dissolved\ S\ = 1.2239\ x \tag{10}$$

$$Dissolved\ Fe = 1.1549\ x \tag{11}$$

Setting the intercept to zero improved the R squared value, however, as seen in Fig. 2, the regression lines for the TA and dissolved Fe data no longer fit the lower concentration data points, requiring the the use of different regression options for these parameters. While a linear regression remained the best fit for the TDS and dissolved S data, a power regression provided the best fit for TA and dissolved Fe data. Although the calculated R-squared values for the non-linear equations more closely approach 1, R is not an appropriate indication of goodness-of-fit for non-linear curves. This is better described by the standard error of regression, or residual standard error (S). A comparison of the R-

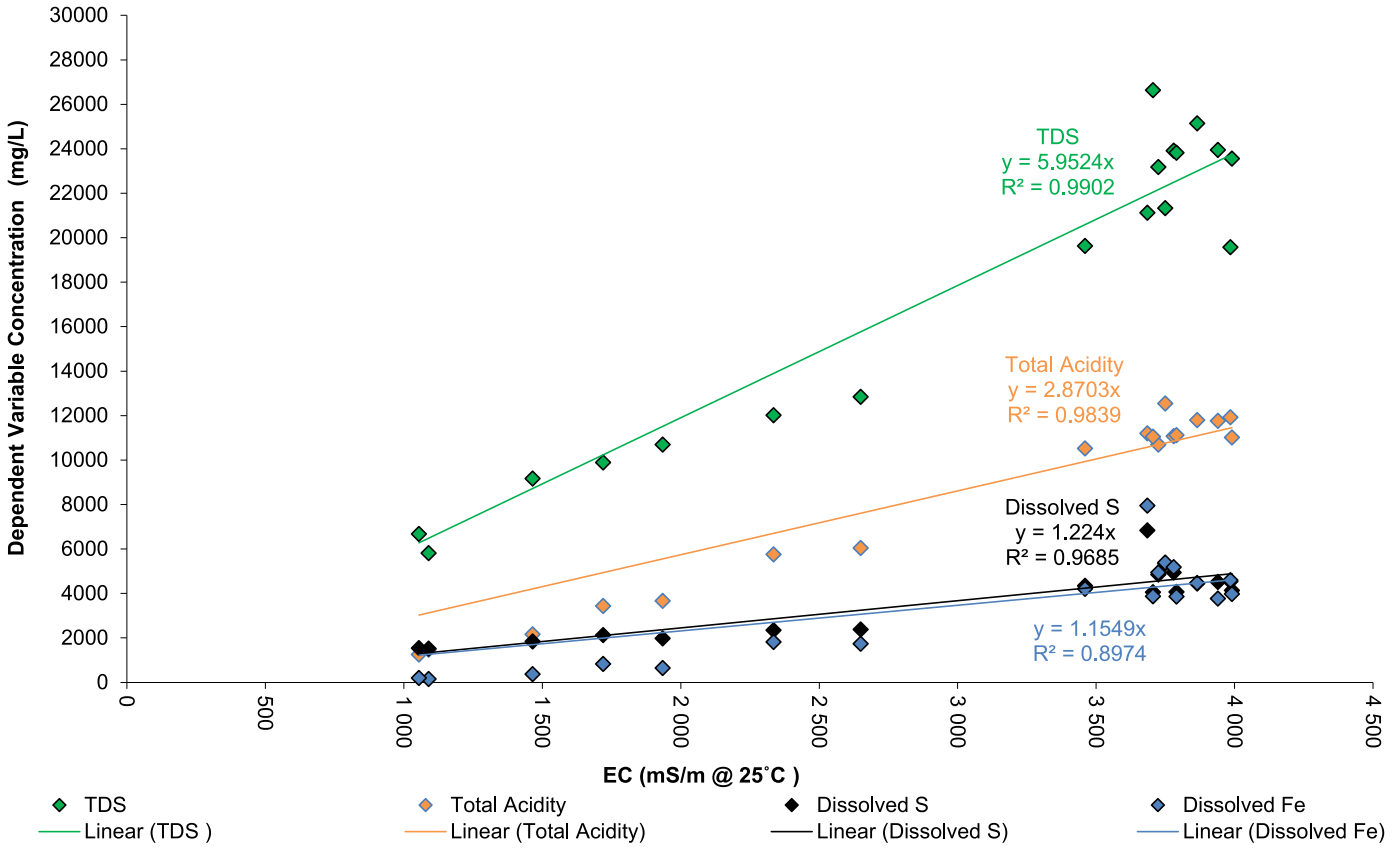


**Fig. 2.** Linear regression equations with the intercept set to zero for total dissolved solids, total acidity, dissolved iron and sulfur as a function of electrical conductivity:

square values achieved for the various mathematical regression equations are given in Table 4, and scatter plots showing the amended power regression lines are shown in Fig. 3.

A visual inspection of the scatter plots indicated the presence of some outlying data points, and further regression analysis was performed, where linear and power residual values were normalized to confirm the rejection of outliers. An iterative process was followed until all outliers were rejected. The output of the statistical analyses are shown in the supplementary data information (Appendix F1 – F4). The rejection of outliers resulted in an improvement in R- square value for all parameters, and these and the revised linear/power regression lines shown in Fig. 4.

Given the significance of the relationship between EC and the selected parameters, and using EC as a proxy, Eqs. 12–15 could be used for prediction of TDS, TA, dissolved S, and dissolved Fe concentrations for the specified sites.

$$\text{TDS} = 5.9804\ x \tag{12}$$

$$TA\ = 0.0127x^{1.6623} \tag{13}$$

$$\text{Dissolved S} = 1.1498\ x \tag{14}$$

$$Dissolved\ Fe\ = 0.000006x^{2.4675} \tag{15}$$

The regression equations were also be used to derive the EC values corresponding to water quality limits for TDS, dissolved Fe and S. This could be useful as a rapid test for compliance, which would then trigger further analysis and appropriate remedial action. The EC values corresponding to the water quality limits for TDS, dissolved S and Fe are as follows:

- EC ≈ 201 mS/m ≈ TDS water quality compliance limit of 1200 mg/L
- EC ≈ 72/145 mS/m Dissolved S – 167/83 mg/L acute health/asthetic water quality compliance limits
- EC ≈ 173 mS/m ≈ Dissolved Fe – 2 mg/L chronic health water quality compliance limit
- TA – water quality compliance limits not allocated

## Conclusions

Comparison of data from two AMD sites in the Mpumalanga coal mining region, against drinking water legislation values, showed that a range of physical and chemical parameters exceeded regulatory limits and could negatively affect certain chemical and biological processes in

**Table 4**
A comparison of the R-squared values achieved for each parameter using the different regression options and after rejection of outliers.

| Parameter | Linear RegressionR-Square value | Linear Regression with zero interceptR-Square value | Power RegressionR-Square value | Linear/Power Regression R-Square value – after rejection of outliers |
|---|---|---|---|---|
| Total Dissolved Solids | 0.9268 | **0.9902** | 0.9576 | **0.9968** |
| Total Acidity | 0.9824 | 0.9839 | **0.9920** | **0.9965** |
| Dissolved S | 0.7794 | **0.9685** | 0.8732 | **0.9904** |
| Dissolved Fe | 0.7764 | 0.8974 | **0.9597** | **0.9748** |

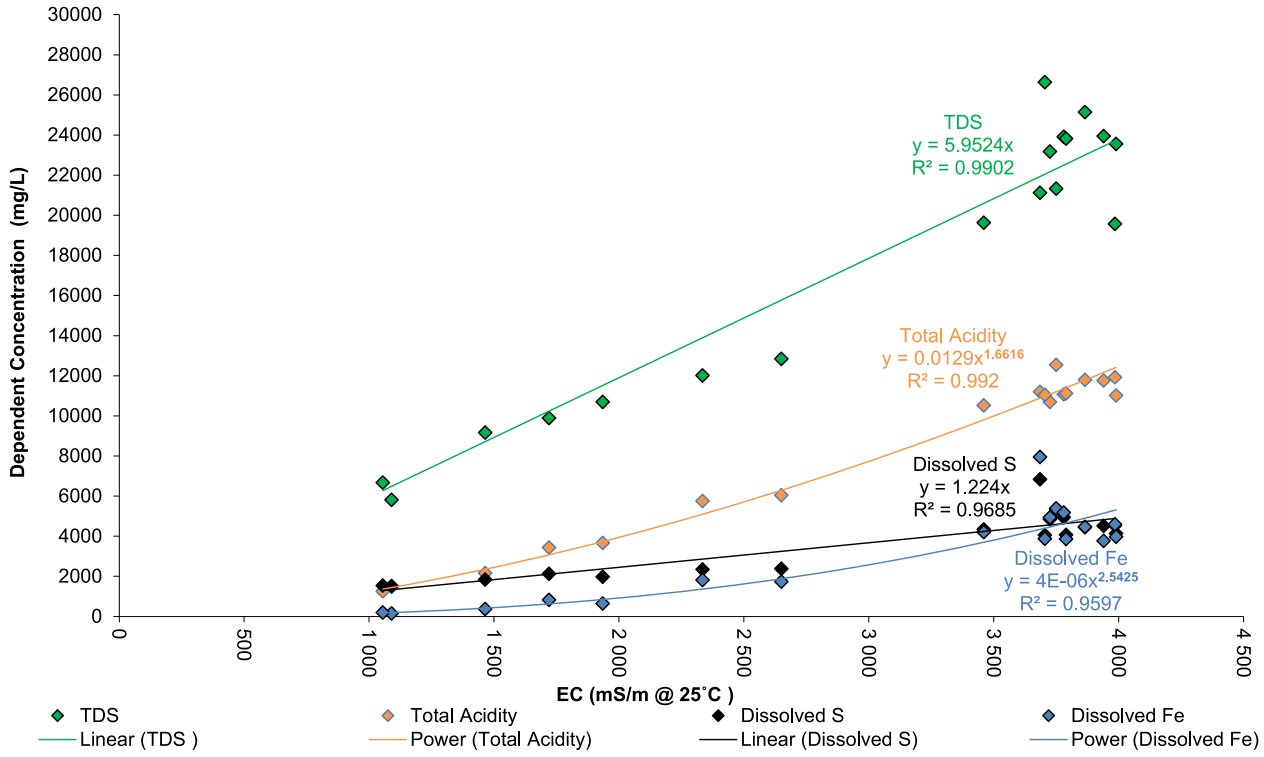


**Fig. 3.** Linear regression with the intercept set to zero, and power regression equations used for total dissolved solids total acidity, dissolved iron and sulfur as a function of electrical conductivity.

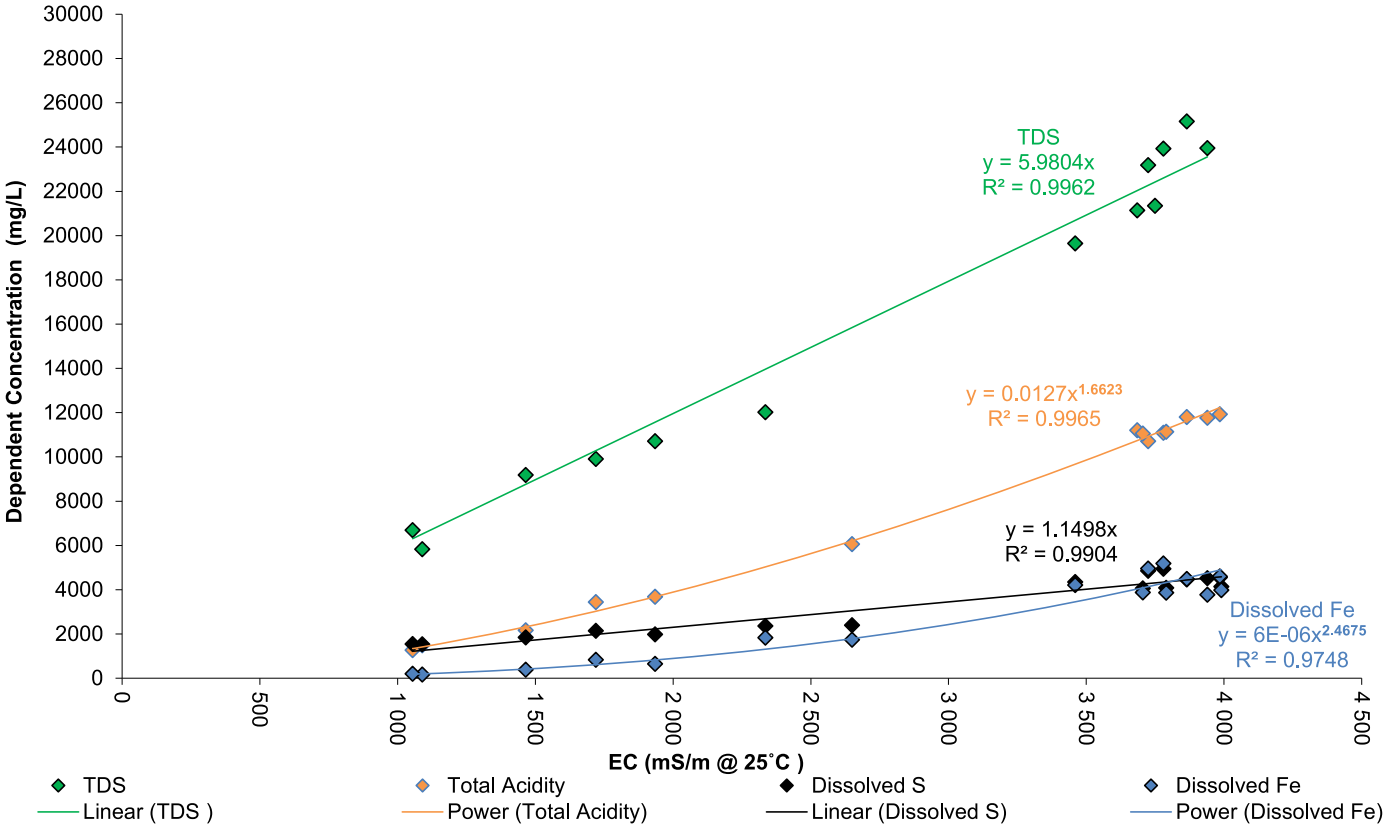


**Fig. 4.** Total dissolved solids total acidity, dissolved iron and sulfur as a function of electrical conductivity: Linear regression with the intercept set to zero, and power regression equations after rejection of outliers.

the surrounding environment, which, in turn would impact, the health of plant, human and aquatic life.

Strong correlations were observed between the major contributing parameters to these AMD waters. Regression analysis confirmed the linear relationship between the dependent and independent variables, and as such, electrical conductivity could be used as a proxy to predict specific paranmeter concentrations in AMD waters using the mathematical equations describing the regression lines.

The regression equations could also be used to calculate the electrical conductivity value corresponding to the water quality limits for total dissolved solids, dissolved iron, and sulfur.

The significance of these relationships lies in the relative ease of electrical conductivity determination and the possibility to predict the concentration of the major contributing elements of a specified acid mine drainage body. Derevation of the electrical conductivity value corresponding to the water quality limits for selected parameters would provide a rapid test for compliance, where exceedance of the calculated threshold electrical conductivity values would trigger a response for further analysis and appropriate remedial action to be taken.

## Recommendations

Acid mine drainage composition is dependent on the geology and environmental conditions which are unique to a particular region, and, as such, the correlations observed for the acid mine drainage sites in this study should not be considered universal. This work is intended as a proof of concept for adaptation at other acid mine drainage sites and individual acid mine drainage sites should be evaluated independently to characterise and establish relationships that might exist between their various parameters.

These relationships should not be viewed as a replacement to continuous monitoring which is required for conformance to respective water use licence conditions, but as a tool that could prove invaluable for a rapid test of compliance, and during disaster events, where the quick turnaround of analysis data would facilitate a faster response time to expedite remedial action necessary to prevent potential environmental damage caused by unintended release of these waters.

Statistical relevance increases as the data pool increases, and continuous monitoring is essential to increase the data pool, and also to identify any significant changes that might occur as a result of chemical changes in an AMD body over time. This should be accompanied by a periodic re-evaluation of the statistical relationships. The availability of a larger pool of data could also facilitate the identification of relationships between other parameters present in specific AMD waters.

## CRediT author statement

**Janet Smith:** Conceptualization, Methodology, Project Management, Investigation, Formal analysis, Data Curation, Visulisation, Writing – Original Draft. **Craig Sheridan:** Conseptulisation, Supervision, Funding, Writing – Review & Editing. **Lizelle van Dyk:** Supervision, Sampling, Writing – Review & Editing **Kevin Harding:** Supervision, Writing – Review & Editing

## Declaration of Competing Interests

The authors declare that they have no known competing financial interests or personal relationships that could have appeared to influence the work reported in this paper.

## Acknowledgments

Thank you to Sasha Naidu and Sean Rossouw for their help with the water sampling, Dr Ansuyah Magan for her insight and technical contribution to the statistical analysis, Professor Kathryn Sole and Mr Stephen Batchelor for document review, technical, and language editing, and Stephen Smith for his assistance with the document format editing.

## Supplementary materials

Supplementary material associated with this article can be found, in the online version, at doi:10.1016/j.envadv.2022.100241.

## References

Akcil, A., Koldas, S., 2006. Acid mine drainage (AMD): causes, treatment and case studies. J. Clean. Prod. 14, 1139–1145.
APHA, AWWA & WEF, 2005. Standard Methods for the Examination of Waterand Wastewater.
Aydin, G., 2015. Forecasting natural gas production using various regression models. Petrol. Sci. Technol. 33, 1486–1492.
Banks, D., Younger, P.L., Arnesen, R.-T., Iversen, E.R., Banks, S.B., 1997. Mine-water chemistry: the good, the bad and the ugly. Environ. Geol. 32, 157–174.
Cheusheva, S., 2019. *Linear Regression analysis in Excel* [Online]. Available. https://www.ablebits.com/office-addins-blog/2018/08/01/linear-regression-analysis-excel/ [Accessed 5 November 2019].
Cravotta III, C.A., Kirby, C.S., 2004. Acidity and alkalinity in mine drainage–practical considerations. In: National Meeting of the American Society of Mining and Reclamation and the 25th West Virginia Surface Mine Drainage Task Force, pp. 334–365. April 18-24, 2004.
Davidson, C. 2003. Catchment diagnostic framework for the Klip River catchment, Vaal barrage, October 1998-September 1999.
DMR, 2017. *Operating Mines in Mpumalanga* [Online]. Department of Mineral Resources of South Africa. https://www.dmr.gov.za/mineral-policy-promotion/operating-mines/mpumalanga [Accessed 6 January 2020].
DWAF, 1996. Department of Water Affairs and Forestry, 1996. In: South African Water Quality Guidelines, second edition, 1. Domestic Use.
DWS, 2017. National Water Act (36/1998) National Norms and Standards for Domestic Water and Sanitation Services V 3 - Final ed. Department of Water and Sanitation.
EPA, 2018. 2018 Edition of the Drinking Water Standards and Health Advisories, EPA 822-F-18-001. Office of Water, U.S. Environmental Protection Agency, Washington, DC.
Gazea, B., Adam, K., Kontopoulos, A., 1996. A review of passive systems for the treatment of acid mine drainage. Min. Eng. 9, 23–42.
Geosciences. 2016. Downloadable Maps, Documents, Files [Online]. Council for Geosciences. Available: http://www.geoscience.org.za/index.php/component/content/article?id=386:downloadable-maps-documents-and-files [Accessed 19 January 2016].
Hannigan, A., Lynch, C.D., 2013. Statistical methodology in oral and dental research: pitfalls and recommendations. J. Dent. 41, 385–392.
Kyeremateng, T. K. 2013. Heavy metal pollution in sediments and water from streams within the damang mine concession.
Larson, T.E., Henley, L., 1955. Determination of low alkalinity or acidity in water. Anal. Chem. 27, 851–852.
Marsden, D., 1986. The current limited impact of Witwatersrand gold-mine residues on water pollution in the Vaal River system. J. S. Afr. Inst. Min. Metall. 86, 481–504.
McCarthy, T.S., 2011. The impact of acid mine drainage in South Africa. S. Afr. J. Sci. 107, 01–07.
MineralscouncilSouthAfrica, 2019. Where coal is mined in South Africa - Mining for Schools. Minerals Council South Africa.
Mursau, A. nd. Regression analysis: Evaluate predicted linear equation, R-squared, F-Test, T-Test, p-Value, etc [Online]. Available: http://cameron.econ.ucdavis.edu/excel/ex61multipleregression.html [Accessed 20 November 2019 ].
Nordstrom, D.K., Blowes, D.W., Ptacek, C.J., 2015. Hydrogeochemistry and microbiology of mine drainage: an update. Appl. Geochem. 57, 3–16.
SABS 2006, 2006. South African National Standards, Drinking Water 2006. In: South African National Standards, Drinking Water 2006, 241. SANS. ISBN 0-626-18876-8.
SABS, 2015. South African National Drinking Water Standard. (SANS), p. 241, 2015.
Simate, G.S., Ndlovu, S., 2014. Acid mine drainage: challenges and opportunities. J. Environ. Chem. Eng. 2, 1785–1803.
Smith, J., Sheridan, C.M., van Dyk, L.D., Harding, K.G., 2021. Seasonal characterisation of acid mine drainage in Mpumalanga coalfields region. In: South African Chemical Engineering Congress 2021, pp. 20–22. September 2021 Virtual. Johannesburg.
Smith, K.S., 2007. Strategies to predict metal mobility in surficial mining environments. Rev. Eng. Geol. 17, 25–45.
Tripepi, G., Jager, K., Dekker, F., Zoccali, C., 2008. Linear and logistic regression analysis. Kidney Int. 73, 806–810.
Tutu, H., McCarthy, T., Cukrowska, E., 2008. The chemical characteristics of acid mine drainage with particular reference to sources, distribution and remediation: the Witwatersrand Basin, South Africa as a case study. Appl. Geochem. 23, 3666–3684.
WRC, 2015. South African Mine Water Atlas. The Water Research Commission.
Yan, X., Su, X., 2009. Linear Regression Analysis: Theory and Computing. World Scientific.